Journal of Alloys and Compounds 509 (2011) 195–199

Contents lists available at ScienceDirect

Journal of Alloys and Compounds

journal homepage: www.elsevier.com/locate/jallcom

Analysis of antiphase domain growth in ternary FeCo alloys after different cooling rates and annealing treatments using neutron diffraction and positron annihilation

Ralph Gilles[a,*], Michael Hofmann[a], Francis Johnson[b], Yan Gao[b], Debashis Mukherji[c], Christoph Hugenschmidt[a], Philip Pikart[a]

[a] *Technische Universität München, ZWE, FRM II, Lichtenbergstr. 1, 85747 Garching, Germany*
[b] *GE Global Research, One Research Circle, Niskayuna, NY 12301, USA*
[c] *Technische Universität Braunschweig, Institut für Werkstoffe, Langer Kamp 8, 38106 Braunschweig, Germany*

ARTICLE INFO

Article history:
Received 10 August 2010
Accepted 14 September 2010
Available online 22 September 2010

Keywords:
Nanostructured materials
Domain structure
Order–disorder effects
Phase transitions
Neutron diffraction
Positron spectroscopies

ABSTRACT

FeCo alloys are industrially important engineering materials which play an outstanding role in applications requiring soft magnetic materials. The challenge is to include ternary elements to improve the mechanical properties. Here noble elements as Pt or Pd were used for these experiments. With neutron diffraction and positron annihilation technique $Fe_{67}Co_{30}Pt_3$ and $Fe_{67}Co_{30}Pd_3$ (at. pct.) samples were measured to study the influence of different cooling rates on ordering and disordering. The ordering and disordering process is responsible for the mechanical properties in dependence of temperature. The correlation of ordering and defect density is described.

1. Introduction

There is a long tradition to use FeCo alloys with ternary element additions as engineering materials due to their soft magnetic properties at high temperatures. FeCo alloys are characterized by low coercivity, high permeability, high tensile strength, high Curie temperature (T_C) and the highest saturation magnetization of all known magnetic alloys. Typical applications are transformer cores, electrical generators/motors, solenoid valves or diaphragms in telephone handsets.

There is an reawakened interest in FeCo alloys due to the increased demands of modern electrical power generation and distribution equipment [1,2]. These demands are especially severe in electrical applications for extreme environments. Then again FeCo alloys pose unique challenges because of their structural and physical properties, especially in nanostructured systems [3].

At room temperature the FeCo alloys are partly ordered depending on the thermal history. An ordered phase leads to decreased ductility leading to mechanical embrittlement. In addition, the ordered alloy is difficult to roll and to machine [4]. Below the T_c temperature Fe and Co will partly distribute into two interpenetrating primitive cubic sublattices and form an ordered B2 type structure. The energetics of FeCo phase tranformations are discussed in Abrikosov et al. [5]. At the stoichiometric composition of this ferromagnetic material the ordered phase B2 has the lowest energy. Without a magnetic contribution to the free energy the succession of phases with respect to energy completely reverses and leads to the lowest energy level for the random disordered bcc A2 phase. In Fe rich FeCo alloys, magnetism stabilizes the bcc structure relative to the close-packed fcc and hcp structure, and the B2 phase originates from the ferromagnetism [6].

Due to the fact that Fe and Co are neighbours in the periodic table it is expected that it costs little energy to exchange Fe and Co antistructure atoms [7]. This conjecture is supported by the low critical temperature of about 730 °C for the transition from the ordered B2 phase to the disordered A2 phase.

The B2 structure type alloys have a few typical characteristics. For example, point defects arising by "anti-structural" and "triple point" mechanisms can lead to vacancies on the two sublattices [8]. Antistructural defects in B2 phases are defined by each A atom occupying a β-site (the wrong site), one B atom occupies an α-site. In triple-defect B2 phases, for each A atom occupying a β-site, two vacancies are formed on α-sites. From theoretical models for the thermodynamic properties of intermetallic B2 phases

---

[*] Corresponding author. Tel.: +49 89 289 14665.
E-mail address: ralph.gilles@frm2.tum.de (R. Gilles).

0925-8388/$ – see front matter © 2010 Elsevier B.V. All rights reserved.
doi:10.1016/j.jallcom.2010.09.075

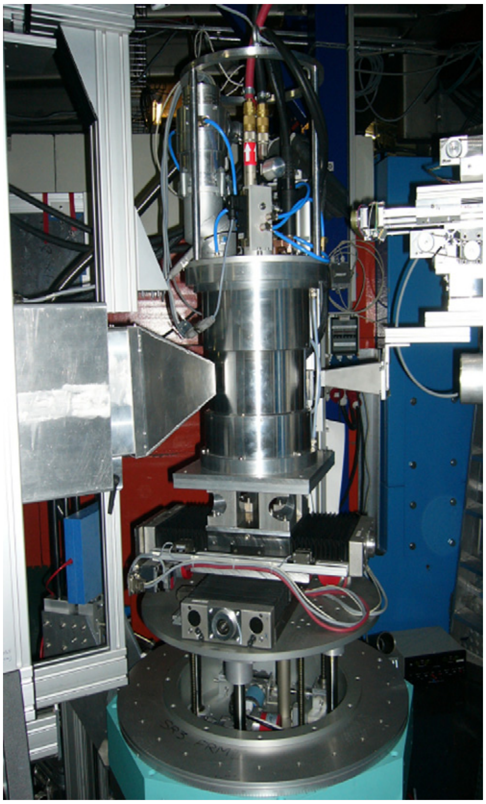

Fig. 1. STRESS-SPEC diffractometer with installed vacuum high-temperature furnace. The neutron beam is coming from right to the left where the detector chamber made of aluminum is seen.

results a small enthalpy for the formation of the substitutional defects, whereas large enthalpy follows for the formation of the triple defects, respectively.

2. Experimental

Cylindrical ingots of $Fe_{67}Co_{30}Pt_3$ and $Fe_{67}Co_{30}Pd_3$ (at. pct.) were prepared by vacuum induction melting with a subsequent heat treatment at 800 °C for 24 h and then different cooling processes were performed. The samples were water quenched (WQ) at a rate of 800 °C/min or air cooled (AC) at a rate of 80 °C/min or furnace cooled (FC) at a rate of 1 °C/min to cool them down from the elevated temperature of 800 °C to room temperature.

As mentioned in a previous study [9] neutron diffraction is the selected method due to the favourable difference in scattering length density of Fe and Co which easily distinguishes between the two elements in a common structure (unlike X-rays). Measurements were performed at the neutron facility Forschungsneutronenquelle Heinz Maier-Leibnitz (FRM II). The high temperature measurements to follow the order–disorder phase transition were performed at the diffractometer STRESS-SPEC [10] equipped with a 2-dimensional area detector covering around 15° in 2θ diffraction angle. This allows to follow the evolution of a superlattice reflection and a fundamental Bragg reflection in the temperature region $T = 25–700$ °C. The samples were mounted in a vacuum high temperature furnace with aluminum windows to avoid air scattering and oxidation of the sample. The furnace was installed on the sample table of STRESS-SPEC just after the collimator and close to the detector (Fig. 1).

Samples with the same cooling rates prepared in thin disc shape of 1 mm thickness were used to study defects in the bulk of the alloy at the Doppler broadening spectrometer of the positron beam facility NEPOMUC which provides the world's most intense low-energy positron beam of about 9×10^8 positrons per second at 1 keV [11,12]. By changing the energy up to 24 keV the penetration depth was varied from the surface up to a depth of around 800 nm. The thermalized positrons can efficiently be trapped in open volume defects such as vacancies before they annihilate with an electron and two 511 keV γ quanta are emitted under an angle of 180°. The electron momentum – the momentum of the thermalized positron is negligible – leads to a Doppler shift of the 511 keV annihilation quanta and hence to a broadening of the annihilation photo peak. The characteristic line shape is described with the S_p parameter (not to be mixed up with the ordering parameter S in diffraction [13]). The S_p parameter is defined from the quotient of counting rate in a fixed area around the maximum and the total counting rate of the 511 keV photo peak. Due to the lower annihilation probability with core electrons in a vacancy than in the perfect lattice the according S_p-parameter is higher.

3. Results and discussion

At the STRESS-SPEC instrument measurements were carried out on the FeCoPt and FeCoPd system which have been cooled each in the three different ways as mentioned above. In Fig. 2 the ordering parameter S – as calculated in Ref. [13] – versus temperature is plotted for these cooling rates. Both systems show very similar behaviour. The FC samples are more or less ordered at RT and have a constant S value up to higher temperature which drops down approaching the T_c temperature. The WQ samples show no ordering (no intensity of the superstructure reflection (1 0 0) is detectable) in the lower temperature region below 400 °C. Above 400 °C the ordering parameter S starts to increase rapidly and decreases again near T_c temperature. The AC samples are a mixture of both profiles. The sample FeCoPd FC seems to order better than the FeCoPt FC sample. This result is in agreement with previous measurements [9]. How the cooling process influences the occupation of the ½ ½ ½ position in the Co sublattice is demonstrated in Fig. 3. The occupation probability is calculated according to Ref. [13] with the assumption of a binary $Fe_{70}Co_{30}$ system. The FeCoPt FC sample reaches the maximum of ordering for Co at RT with a value around 0.55 occupation probability (theoretical highest value by neglecting the ternary element is 0.60). The value of the WQ sample is slightly higher than the FC one with a value of $S = 0.59$ in the maximum near 550 °C. It is clearly visible that in the low temperature region the cooling process is the dominant factor for the degree of order. At a certain temperature all samples start to order and if enough time is available they order up to the maximum degree of order. Close to the T_c temperature all samples completely disorder. The influence of the ternary element on the heating process of the alloy manifests itself in the achieved T_c temperature which is for all ternary compositions specific and independent on the performed cooling rate.

Previous studies [9,14] correlate the ordered structure with the creation of antiphase domains. Heating up the sample induced a growth of antiphase domains. Fig. 4 shows the evolution of the domain size versus temperature for the two ternary alloys. The domain size was estimated using the Debye–Scherrer formula [15]. FC samples have the largest size at RT with 22 nm for FeCoPt and 12 nm for FeCoPd. The AC samples yield at RT in very small sizes below 5 nm in both ternary alloys. In WQ samples because of the lack of visible superstructure reflections no domain size estimation is possible at ambient temperature. Up to 450 °C for both alloys no observable change in the domain size is detectable. However, above 450 °C, the domains of WQ and AC samples grow in a rapid way much faster than the already larger domains of the FC samples. Just before T_c temperature the domain size of all three differently cooled samples from one ternary alloy composition are quite similar.

To receive more information on the domain growth three samples of the FeCoPd system were annealed at three different fixed temperatures of 432 °C, 477 °C, and 500 °C. In Fig. 5 the domain size versus the square root of the annealing time is displayed. The fit of the domain sizes versus time for each annealing temperature results in a gradual domain coalescence $L \sim t^{1/2}$ in agreement to references as Rogers et al. [16]. The results of the in situ heating up to T_c temperature and the annealing at a constant temperature lead to the conclusion that domain size and domain growth depend strongly on the thermal cooling history as well as the dwell temperature and heating rate.

Positron measurements were performed to understand more in detail the structural arrangement of Fe and Co in the sublattices and at the antiphase domain boundaries after various cooling processes. At the Doppler broadening spectrometer of NEPOMUC the

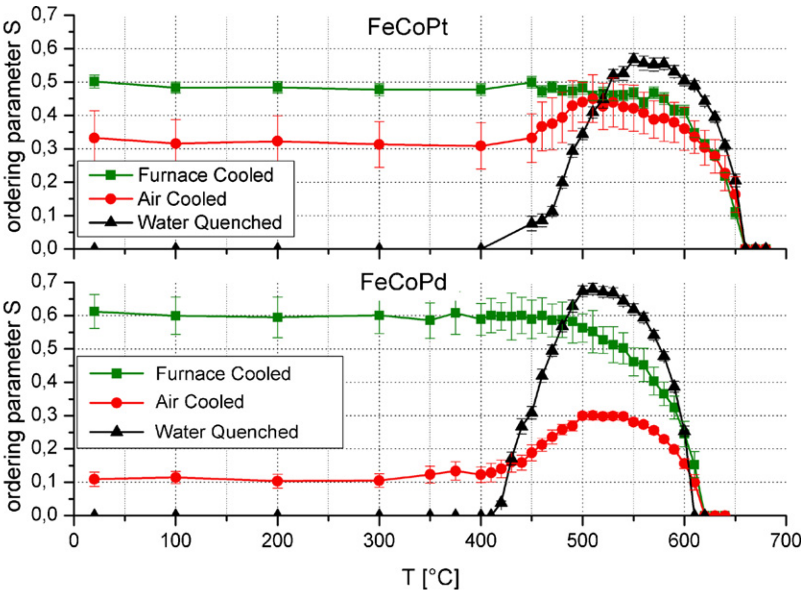

Fig. 2. Ordering parameter *S* versus temperature up to the transition temperature T_c for FeCoPt and FeCoPd samples with different cooling rates (see text).

defect concentration was measured at RT for FeCoPt and FeCoPd. The S_p parameter, introduced above, versus energy (a measure of penetration depth) is depicted in Fig. 6 showing the influence of the defect concentration on the surface and especially in the bulk. Again we want to stress that the S_p parameter is not to be confused with the ordering parameter *S*, rather it is a measure of the defect concentration. For our study the bulk information is more relevant to get volume sensitive information of the alloys. In the higher energy region ($E > 17$ keV) for both alloys the WQ and AC samples have a similar low S_p parameter in contrast to the high S_p parameter in the FC samples. The lower S_p parameter of the WQ and AC samples is attributed to a significant lower defect concentration – mainly coming from "frozen in vacancies" by quenching – than the FC samples. In B2 intermetallic compounds as NiAl or CoAl very large vacancy concentrations were detected on the Ni or Co sublattices in slowly cooled specimens, and these vacancies were attributed to be mainly structural vacancies [17]. This assumption is verified by a theory of vacancy formation in highly ordered non-stoichiometric bcc alloys using the nearest-neighbour bond-energy model [17]. The higher defect concentration of the FC samples have to be mainly correlated to the formation of the domain boundaries of the antiphase domains and in addition to vacancies in the Co sublattice created by the non-stoichiometric composition.

Due to the fact that in WQ and AC samples only a part of the sample is ordered and a large fraction of the sample is disordered the number of antiphase domain boundaries is significantly smaller than in FC samples. As the measurements have shown that the FC samples have larger antiphase domains and a higher defect concentration, it leads to the conclusion that the defects are at the antiphase domain boundaries. The strong effect on the S_p parameter points to vacancies as the main defect. The results matches well with the high order in the domains itself where mainly antisite

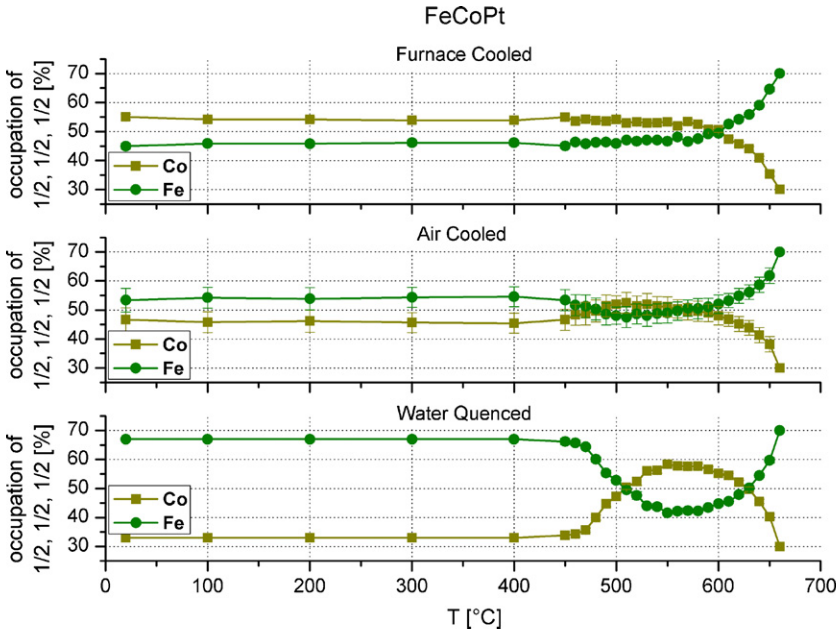

Fig. 3. Occupation of the Co-sublattice position ½ ½ ½ versus temperature in the FeCoPt alloy with different cooling rates.

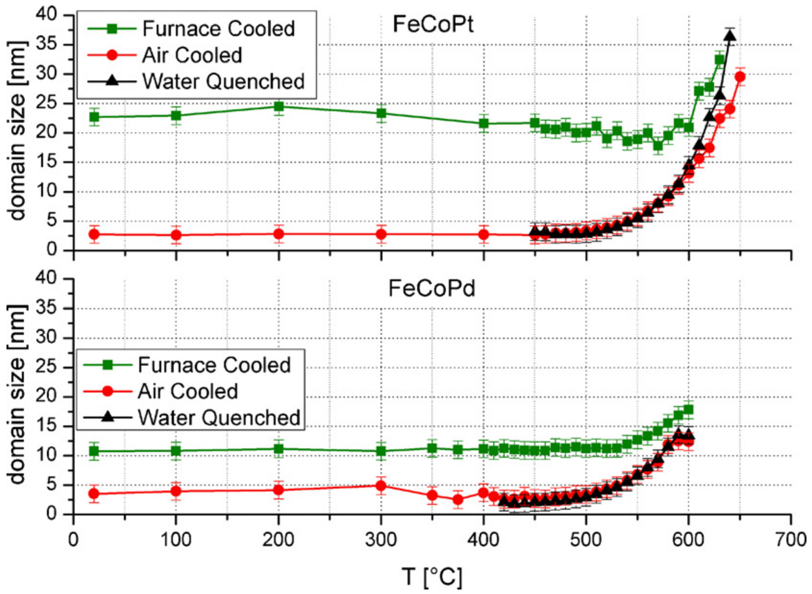

Fig. 4. The growth of the antiphase domains is plotted against temperature up to the respective T_c temperature.

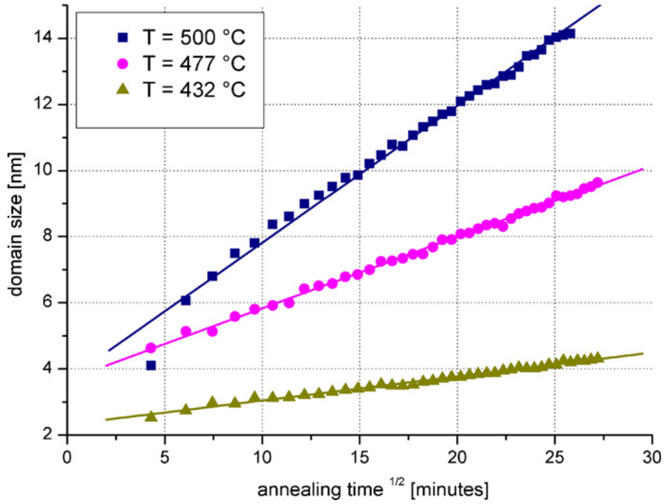

Fig. 5. Domain size versus time for different constant annealing temperatures 432 °C, 477 °C and 500 °C for FeCoPd. The domain sizes were calculated from the integral breadth of the (1 0 0) reflection as in [9].

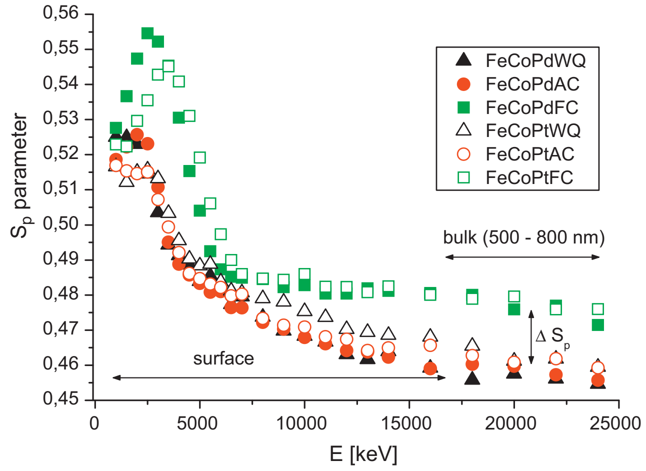

Fig. 6. The defect concentration related S_p parameter versus energy for the FeCoPt alloy and FeCoPd with different cooling rates. The energy is proportional to the penetration depth of the positron beam.

defects (exchange of Fe and Co) are present which can be detected only with the neutron diffraction method but not with positrons.

Since the typical positron diffusion length is in the order of 100 nm and hence about a factor of 20 larger then the mean domain size, positrons would be trapped efficiently in open volume defects at the antiphase domain boundaries. For this reason, the presence of vacancies at the domain boundaries explains the significantly higher S_p parameter observed in the FC samples. In the bulk of the sample the difference of the S_p parameter is 4% in the FeCoPt alloy and 6% in the FeCoPd alloy, respectively. Such differences are normally related to vacancies and not to dislocations or simple antistructural defects. The binary FeCo system with stoichiometric composition has a formation enthalpy of $-\Delta H_f = 10\,\mathrm{kJ\,g\,atom}^{-1}$. Values of $-\Delta H_f$ smaller than $30\,\mathrm{kJ\,g\,atom}^{-1}$ exhibit substitutional defects, whereas B2 phases with $-\Delta H_f$ larger than $30\,\mathrm{kJ\,g\,atom}^{-1}$ exhibit predominantly triple defects [8]. The results of our study seem to contradict the result of Neumann who categorizes FeCo into the substitutional defect group. From the positron measurements we detect a larger number of vacancies in the FC samples due to higher defect densities at the antiphase domain boundaries. The domain boundaries can move only by lattice diffusion processes including the exchange of sites of atoms and vacancies. The antiphase domain boundary migration depends on the available vacancies at the boundary and their mobility. Activation energy measurements of antiphase domain coalescence on FeCoV samples result in similar values as volume diffusion in disordered material and much lower values as expected for the ordered material. This is a hint to a substantially disordered environment of mobile vacancies in the moving antiphase domain boundaries [18]. The assumption of the large vacancy number in the sublattice of Co is supported by measurements on the pure elements and the binary alloy with positrons. The surrounding of the defects described in these measurements results in that Fe atoms are around the defects, which means that the vacancy defects are in the Co sublattice. The value of the defect concentration of the FC sample seems to be influenced by the ternary element if both alloys are compared. Due to the low concentration of only 3% of the ternary addition it is, however, very difficult to see the influence of the ternary element on the whole defect concentration profile (Fig. 6).

The ordering transformation in FeCo involves an increase in the lattice constant in the order of 0.2% [13]. Measurements of the lattice parameters in the differently cooled FeCoPt and FeCoPd samples generally resulted in smaller lattice constants of FC samples, which supports the assumption of the higher defect concentration in these samples.

4. Conclusion and outlook

Neutron diffraction experiments and positron measurements of ternary FeCoPt and FeCoPd alloys allow detailed information on the mechanism of order and disorder as function of thermal history (e.g. cooling rates). The cooling rate has strong influence on the degree of order at room temperature. A more or less fully ordered or disordered state is possible by adjusting the cooling rate. Heating up to just below the T_c temperature always leads to a high degree of order of the alloy before crossing the T_c temperature whereupon complete disorder occurs. The antiphase domains created when the alloy's order grows with a rate directly dependent on the annealing temperature. Especially, the influence of the ternary element to the T_c temperature is clearly pointed out. Neutrons allow in-situ monitoring of the site occupation of the two main elements, Fe and Co. The positron measurement shows higher defect concentrations for the FC samples which is connected to the creation of vacancy defects at the antiphase domain boundaries, especially in the Co sublattice because of the non-stoichiometric composition.

Further measurements on the binary alloys $Fe_{70}Co_{30}$ and $Fe_{50}Co_{50}$ are foreseen to gain more detailed information on the mechanism including the ternary element of various alloys. It is planned to measure with positrons the defect concentration in-situ while heating up the samples to the T_c temperature. This will allow comparison of the annealing of defects and the influence of antiphase domains over the full temperature range. Theoretical calculations of the stoichiometric FeCo samples yield an indication that the interaction of chemical and magnetic order plays a key role in the formation of the ordered B2 phase.

Acknowledgments

The authors would like to thank Alexander Schmidt and Manfred Teufelhart for support on the high-temperature furnace, Jens Krueger for support on the temperature control and Christian Randau and Lukas Karge on the evaluation process.

References

[1] T. Sourmail, Prog. Mater. Sci. 50 (2005) 816–880.
[2] R.S. Sundar, S.C. Deevi, Int. Mater. Rev. 50 (2005) 157–192.
[3] A. Diaz-Ortiz, R. Drautz, M. Fähnle, H. Dosch, J.M. Sanchez, Phys. Rev. B 73 (2006), 224208-1–224208-15.
[4] K. Kawahara, J. Mater. Sci. 18 (1983) 3437–3448.
[5] I.A. Abrikosov, P. James, O. Eriksson, P. Söderlind, A.V. Ruban, H.L. Skiver, B. Johansson, Phys. Rev. B 54 (1996) 3380–3384.
[6] C.L. Fu, Phys. Rev. 52 (5) (1995) 3151–3158.
[7] N. Neumayer, M. Fähnle, Phys. Rev. B 64 (2001), 132102-1–132102-4.
[8] J.P. Neumann, Acta Metall. 28 (1980) 1165–1170.
[9] R. Gilles, M. Hofmann, Y. Gao, F. Johnson, L. Iorio, M. Larsen, F. Liang, M. Hoelzel, B. Barbier, Metall. Mater. Trans. A 41A (2010) 1144–1150.
[10] M. Hofmann, R. Schneider, G.A. Seidl, J. Rebelo-Kornmeier, R.C. Wimpory, U. Garbe, H.-G. Brokmeier, Physica B 385–386 (2006) 1035–1037.
[11] C. Hugenschmidt, B. Löwe, J. Mayer, C. Piochacz, P. Pikart, R. Repper, M. Stadlbauer, K. Schreckenbach, Nucl. Instrum. Methods Phys. A 593 (2008) 616–618.
[12] C. Hugenschmidt, G. Dollinger, W. Egger, G. Kögel, B. Löwe, J. Mayer, C. Piochacz, P. Pikart, R. Repper, K. Schreckenbach, P. Sperr, M. Stadlbauer, Appl. Surf. Sci. 255 (2008) 29–32.
[13] D.W. Clegg, R.A. Buckley, Met. Sci. J. 7 (1973) 48–54.
[14] R.A. Buckley, Met. Sci 9 (1975) 243–247.
[15] B.E. Warren, X-ray Diffraction, Dover Publications, Inc., New York, 1990, ISBN 0-486-66317-5.
[16] J.A. Rogers, H.M. Flower, R.D. Rawlings, Met. Sci. 9 (1975) 32–35.
[17] S.M. Kim, Phys. Rev. B 33 (2) (1986) 1509–1511.
[18] A.T. English, Trans. Metall. Soc. AIME 236 (1966) 14–18.